13th World Conference on Earthquake Engineering
Vancouver, B.C., Canada
August 1-6, 2004
Paper No. 773

ENHANCING DYNAMIC PERFORMANCE OF LIQUID STORAGE TANKS BY SEMI-ACTIVE CONTROLLED DAMPERS

Hirokazu Iemura [1] and Akira Igarashi [2] and Afshin Kalantari [3]

SUMMARY

This paper deals with the behavior of cylindrical liquid storage tanks facilitated by different passive, hybrid passive and semi-active control with base isolation systems to enhance the performance of this type of structures and to show the merits of variable dampers. The cases of linear base isolation with viscous damping, a base isolation system with bilinear behavior and viscous damping, and a linear base isolation system together with a variable damper are investigated. In the last case, semi-active control has been applied to control the variable damper using the pseudo negative stiffness algorithm which was previously proposed by the authors. A lumped mass numerical model of the tank and the contained liquid has been employed in the analysis. Height of sloshing, base shear and displacement of the tank during the excitation are considered as the indices representing the dynamic performance of the tank. For different dynamic characteristics of the systems, namely isolation period, damping ratio of the isolation system and gain factors in pseudo negative stiffness algorithm, the optimum values for the base devices are obtained by minimizing these performance indices for a variety of ground motions. The base shear of the tank, as well as the structural displacement and the sloshing of the liquid during different ground motions dramatically reduced by using the semi-active control algorithm together with base isolation systems.

INTRODUCTION

The liquid storage tanks is one of the important elements of the lifeline and industrial systems now in the world and any damage to these structures during earthquakes can cause a severe social, economical or environmental problem. Reviewing recent destructive earthquakes shows that liquid tanks have shown improper performance, for example, during Nihon Kai-chu bu (1983), Izmit (1999) and Tokachi-Oki

[1] Professor, Department of Civil Engineering Systems, Kyoto University, Yoshida Honmachi, Kyoto 606-8501, Japan, e-mail: iemura@catfish.kuciv.kyoto-u.ac.jp

[2] Associate Professor, Department of Civil Engineering Systems, Kyoto University, Yoshida Honmachi, Kyoto 606-8501, Japan, e-mail: igarashi@catfish.kuciv.kyoto-u.ac.jp

[3] Ph.D. Student, Department of Civil Engineering Systems, Kyoto University, Yoshida Honmachi, Kyoto 606-8501, Japan, e-mail: aphsheen@catfish.kuciv.kyoto-u.ac.jp

(2003) earthquakes. Uncontrolled overturning loads causes settlement at the foundation and buckling of the steel tanks at the base. Severe sloshing responses have caused damage to the tanks or fire in naphtha tanks in refineries.

On the other hand the amount of the capital now invested in the lifelines and infrastructures in some urban areas suggests the importance of implementing more capable and intelligent protection systems against earthquake for them. For example, just in case of occurring the probable "Nan kai" earthquake in Japan, the economical loss is predicted to be as much as 53 to 81 billion Japanese Yen.[6]

Parallel to increasing of investment of the public budget to construction of infrastructures, the society demand of providing services with more safety also increases. To answer this demand, it is required to apply new technologies and science in the practical field. Innovations in digital technology have changed the definitions and boundaries of the field of civil engineering in recent years. Ideas of passive, active and semi active vibration control of structures provided a wide area of research and brought a huge amount of success in research and practice in this field.

Although passive control systems can provide considerable response reduction effects in the structures, there were still uncertainties on the real performance of the structures facilitated by these instruments. Modern ideas proved to be effective in improving the seismic performance of structures since the active control idea was applied for the first time to a real structure in Tokyo in 1989. [7] However, still several issues appeared unsolved by actively controlled systems such as how to provide energy demanded by these systems at the hazardous moments or how to provide reliable control systems and algorithms such that both overcome strong earthquakes and they be feasible to apply. With regard to these points, intelligent energy absorbing mechanisms – semi-active systems - appeared to have a great efficiency.

Since the idea of structural active control was taken from the mechanical and electronic engineering fields, the associated classic and modern algorithms have been adopted for active control of civil engineering structures. For semi active control methods, also the concept of clipping of the commands produced by the same algorithms is utilized to control the variable device. The requirement of multi-inputs

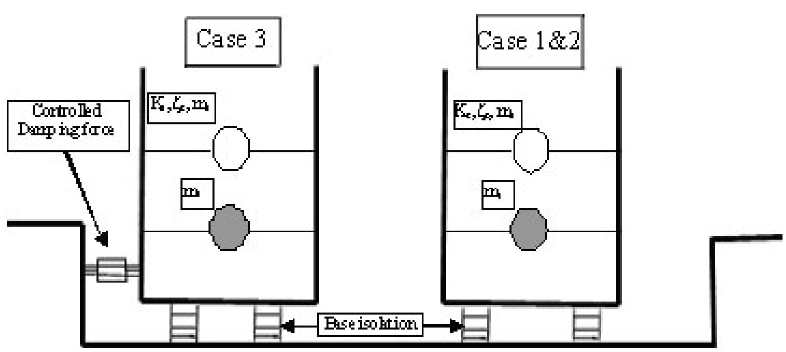

Figure 1) Dynamic model of the studied system

to the algorithm ends with the need for installing several sensors in the structure which increases both the complicacy and cost of the control.
Therefore, application of simpler autonumous- decentralized algorithms should be under more consideration in recent years.

This study deals with design and applying an autonomous decentralized single-agent semi-active control system to the liquid storage tanks by the name of Pseudo Negative Stiffness algorithm (PNS) that delivers high levels of mission reliability in dynamic and rapidly changing environments such as earthquake. The control is applied in the combination with the base isolation and results are compared with passive base isolation methods and with a system without any control.
In this study, three different base isolation systems described in Figure 1 are studied in order to compare the response objectives in each case; Base isolation system with a parallel behavior of linear spring and viscous damping (case 1), bilinear base isolation with a hysteretic behavior (case 2) and linear base isolation system along with semi actively controlled variable damper (case 3).

MODEL OF THE LIQUID TANK

In the dynamic models of rigid liquid tanks containing liquids which have been already presented, the tank and the contained liquid are modeled as some discretized lumped masses. Some of these models have been presented by Veletsos [1], Haroun [3] and Housner [4]. During these studies, it has been shown that the sloshing part of the liquid can be expressed as the combination of different modes with quite long periods. Wang et. al. [10] calculated accumulated percentage of modal participation factors with respect to the height to radius ratio (H/R), to show that for H/R>0.6, over 95 percent of the hydrodynamic response is sufficiently covered by the first mode.
The model proposed by Housner for cylindrical tanks is used in this study, where just the first sloshing mode has been modeled by a lumped mass-spring system (Figure 2).

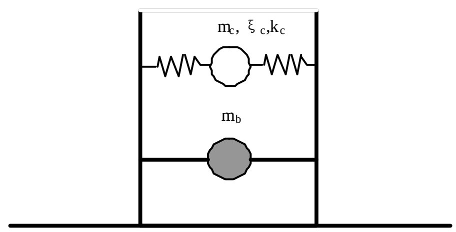

Figure 2) The Housner lumped mass model for liquid storage tank

The parameters of this model are:

$$m_c = M_l \times (0.6) \times \frac{\tanh(1.8\frac{H}{R})}{1.8\frac{H}{R}}$$

$$k_c = 5.4 \times \frac{m_c^{\,2}.g.H}{M_l R^2}$$

$$m_i = \frac{M_l . \tanh(1.7\frac{R}{H})}{1.7\frac{R}{H}}$$

$$T_c = 2\pi\sqrt{\frac{m_c}{k_c}}$$

where H and R are the height and radius of the cylindrical tank respectively, m_c is the convective mass, m_i is the impulsive mass of the liquid, k_c is the spring attached to the convective mass, $M_l=m_c + m_i$, and g is the gravity acceleration.

RESPONSE CONTROL SYSTEMS

Case 1

In this case, the force - deformation behavior of the bearing is supposed to be linear. A linear elastic spring is considered to work in parallel with a dashpot which can be a numerical model of laminated rubber bearings accompanied by some viscous damping devices shown in the Figure 3:

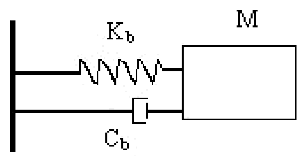

Figure 3) Response control system in case 1

The restoring force produced by such a bearing can be calculated as F_b such that:

$$F_b = K_b u_b + C_b \dot{u}_b$$

Where K_b and C_b are the stiffness and damping coefficient of the base isolation system, respectively, u_b and $\dot{u}_b$ are the displacement and velocity of the structure at the base. By these definitions, natural period of the system is defined as:

$$T_b = 2\pi\sqrt{\frac{M}{K_b}}$$

And damping coefficient is calculated as:

$$C_b = 2hM\omega$$

where h is the damping ratio base and ω is the natural frequency of the base isolation.

Case 2

In this case the force - deformation behavior of the bearing is supposed to be nonlinear. A hysteresis behavior is modeled employing the relation introduced by Park and Wen [9] which can be a numerical model of lead-core rubber bearings (LRB), friction pendulum bearings (FPS) or high damping rubber bearings (HDRB). In this case the lead core rubber bearings are modeled.

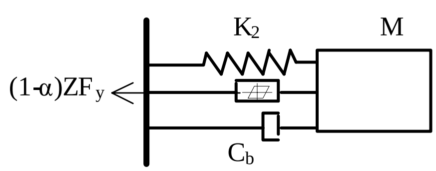

Figure 4) Response control system in Case 2, $K_2=\alpha K_1$

The restoring force produced by such a bearing can be calculated as F_b such that:

$$F_b = \alpha K_1 u_b + C_b \dot{u}_b + F_z$$
$$F_z = (1-\alpha) F_y Z$$

Where K_1 is the pre-yield stiffness of the base isolation system α is the ratio of post to pre yield stiffnesses, F_y is the yield force. The symbols u_b and $\dot{u}_b$ denote the displacement and velocity of the structure at the base. By these definitions, the primary natural period of the systems is defined as:

$$T_b = 2\pi \sqrt{\frac{M}{K_1}}$$

where $K_1 = \frac{F_y}{u_y}$ and damping coefficient is calculated as:

$$C_b = 2hM\omega$$

The hysteresis component Z is a value in the domain of [-1, +1] which is produced by the following differential equation [9]:

$$u_y \dot{Z} = -\gamma |\dot{u}| Z |\dot{Z}|^{n-1} - \beta \dot{u} |Z|^n + A\dot{u}$$

In this equation, β, γ ,A and n are the constants defining the shape of the hysteresis loop and controlling the behavior of model. During the analysis and design, these constants are defined so that $\frac{dZ}{du} = \frac{(1-\alpha)Fy}{u_y}$, where u_y is the displacement of the bearing at the yield point. An overall result of this F_b is shown here in Figure 5:

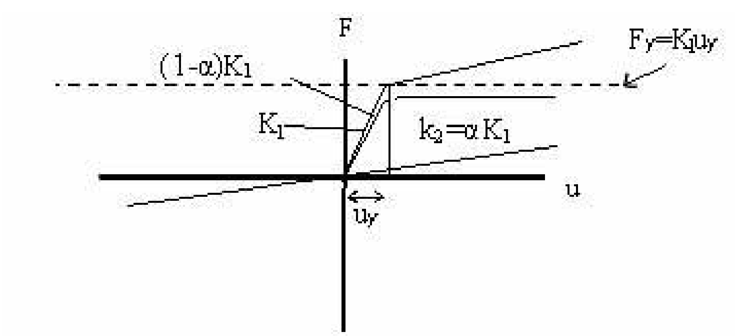

Figure 5) Bilinear load produced by Hysteresis component Z

Case 3

In case 3, a hybrid system consisting of a linear elastic element as the base isolation and a semi-active damper is proposed. In this study, an autonomous decentralized semi-active algorithm by the name of Pseudo Negative Stiffness has been employed in order to control the variable damper. The force produced by this hybrid system then becomes:

$$F_b = K u_b + C \dot{u}_b + F_d$$

Where F_d is the load produced by variable damper following PNS algorithm. K and C are the characteristics of the base isolator.

Semi active control by Pseudo Negative Stiffness algorithm

The pseudo-negative stiffness algorithm [5] describes the applied damping in such a manner that the hysteresis loop produced by the combination of the elastic element and the variable damper can cover a large area in the load-displacement response, providing large energy dissipation with the behavior like rigid perfectly plastic.

Supposing a single-degree-of-freedom system, application of this algorithm allows the increased damping ratio up to 0.534 without increasing the response of the system, comparing with the linear case in which the added damping can cause larger response of the system up to 1.46 times the elastic force. [8]

The control strategy to produce this load has been shown schematically in Figure 6 and can be calculated using the following equation:

$$\begin{cases} F_d = [K_d \quad C_d] \times \begin{Bmatrix} u \\ \dot{u} \end{Bmatrix} & \text{if } F_d \times \dot{u} > 0 \\ F_d = 0 & \text{if } F_d \times \dot{u} > 0 \end{cases}$$

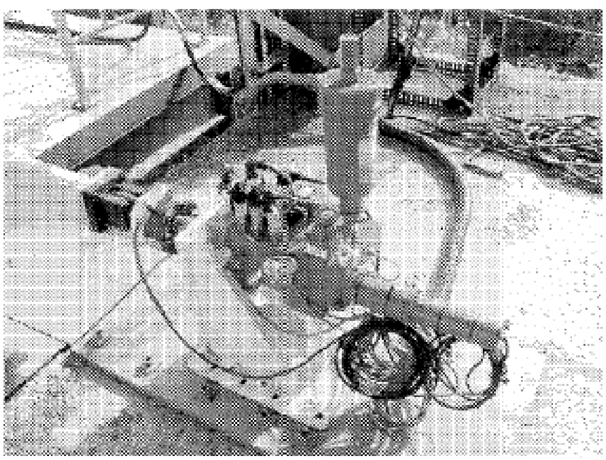

Photo 1) Variable oil damper [5]

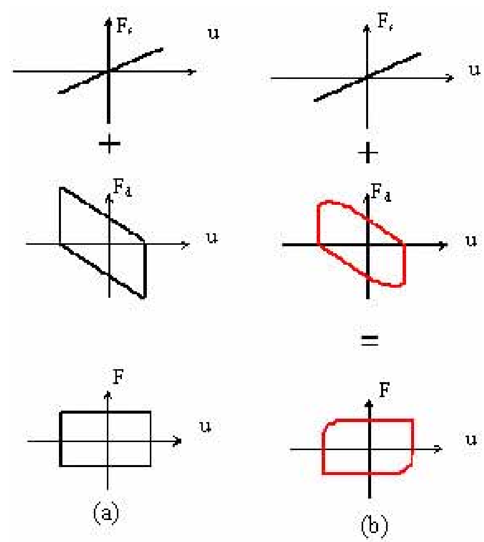

Figure 6) Ideal load (F_d) produced by (a) algorithm, (b) Damper load

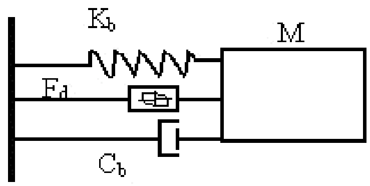

Figure 7) Case 3

where K_d and C_d are the negative stiffness and damping coefficient, respectively and u and $\dot{u}$ are relative displacement and velocity of the damper, respectively. As can be seen in the equation above, the algorithm needs just the data at the location of the damper and this will cause the simplicity of control and reduction of cost of implementation comparing with other algorithms which need to install sensors at different

locations. Such a simple algorithm can produce an *artificial nonlinear damping force* which maximizes the area of the hysteresis loop.
Iemura et. al. carried out tests with a variable oil damper (Photo 1) and successfully produced the pseudo negative stiffness load [5] as shown in Figure 7.

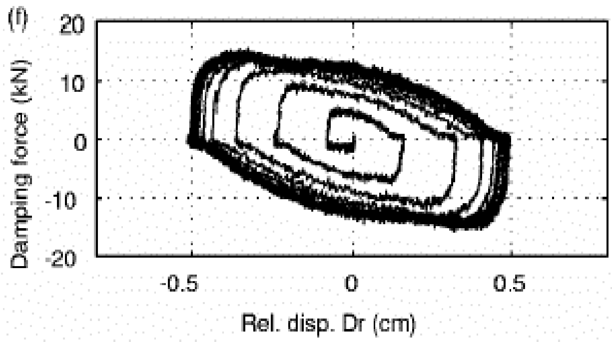

Figure 7) Response of variable damper controlled by Pseudo negative stiffness algorithm subjected to sinusoidal load (1.8 Hz, Max 10 gal) [5]

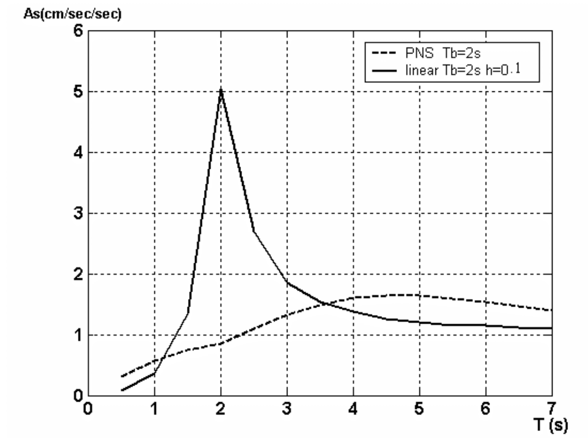

Figure 8) Effect of PNS control on natural period of a SDOF system

The PNS control is shown to elongate the natural period of the system. In Figure 8, the horizontal axes represents the period of harmonic excitation force and the vertical axes represents the acceleration response amplitude of a unit mass to the harmonic load with unit amplitude. The dashed line represents the response of a linear system with PNS controlled variable damper. The natural period of the system is 2 seconds and it can be seen in the figure that adding PNS control reduced the value of the peak of resonance curve as well as elongating the natural period. Although installation of a PNS damper can increase the displacement response due to the excitation, proper implementation of damping produced by the damper, achieves efficient energy absorption with well-limited displacement response.

NUMERICAL STUDY

Cylindrical tanks with the height of 5m and the radius of 3m, installed with the three types of base isolation systems are used for the numerical response analysis, to investigate the performance of the base isolation/control systems. Base shear, displacement of the structure, the ratios of dissipated energy to the input energy, and the vibration energy of sloshing liquid are compared as the performance indices.
Numerical response analysis is carried out using two acceleration records, El Centro (1940) with the maximum acceleration of 342 gal and Kobe (1995) with the maximum acceleration of 814 gal.
The parameters of the base isolation and control system are selected based on a numerical study to minimize the previously mentioned performance.
In each case the parameters are determined as follows:
Case 1) T_b=2s h=0.30
Case 2) $T_b=2s$ h=0.10 F_y/W=0.05, $W=Mg$
Case 3) $T_b=2s$ h=0.02 $K_d=-K$ $C_d = 0.5\frac{K}{\omega}$, $\omega = \frac{2\pi}{T_b}$ K=stiffness of the base isolation.

The sloshing natural frequency or the natural frequency of vibration of convective mass is calculated as:

$$\omega_c = \sqrt{\frac{k_c}{m_c}}$$

Considering the tank dimensions, this value of ω_c is approximately 2.4 Rad/Sec in this case.

RESULTS

The results of response analysis of the controlled tanks under the NS component of El Centro 1940 ground motion are presented. First the base shear produced in each case is shown in Fugure 9. It is shown that the ratio of the base shear F_s to weight W is approximately 0.09 both in cases 1 and 2, and 0.07 in case 3, respectively. It should be noted that the base shear is daramatically reduced comparing with the fixed case.

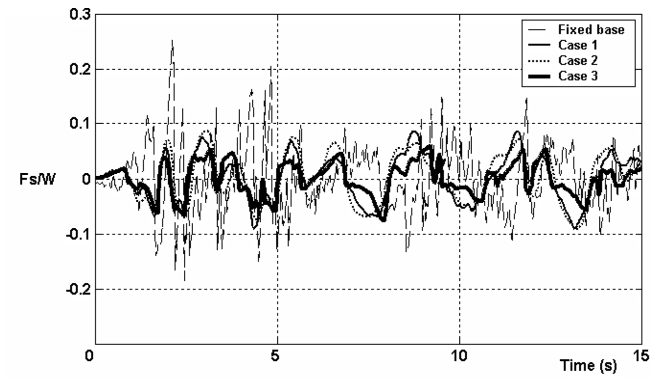

Figure 9) Time history of base shear in three cases and the response of the tank with fixed base (El Centro 1940 342 gal)

Figures 10, 11 and 12 show the base shear displacement hysteresis loops produced by base isolation system in case 1, 2 and 3, respectively.

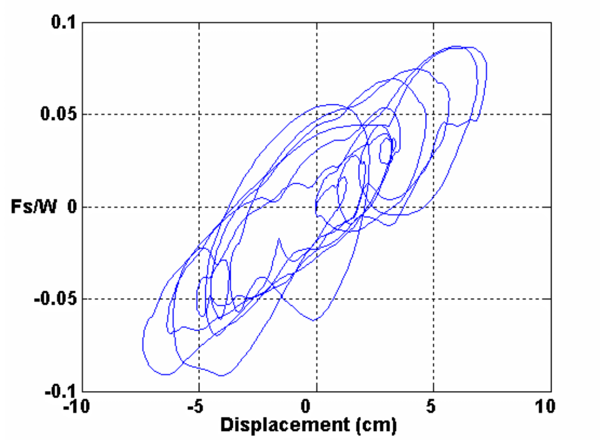

Figure 10) Hysteresis loop, Case 1 (El Centro 1940- 342 gal)

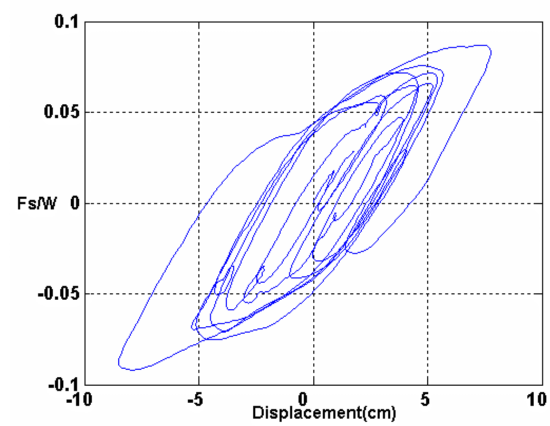

Figure 11) Hysteresis loop, Case 2 (El Centro 1940- 342 gal)

These figures clearly show the behavior of three cases explained in the previous part. Figure 12 shows the hysteresis behavior in case 3 and figure 13 presents the artificial nonlinear damping force produced by PNS algorithm under the El Centro ground motion.

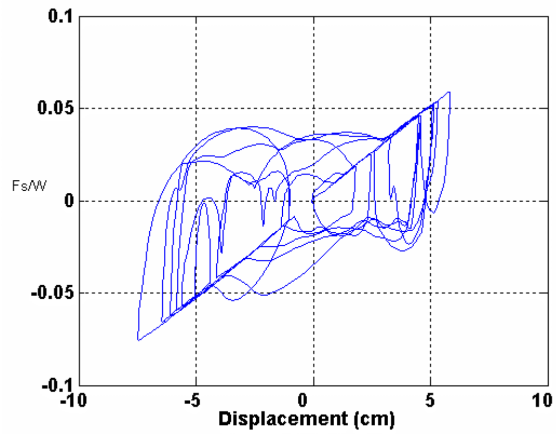

Figure 12) Hysteresis loop, Case 3

(El Centro 1940- 342 gal)

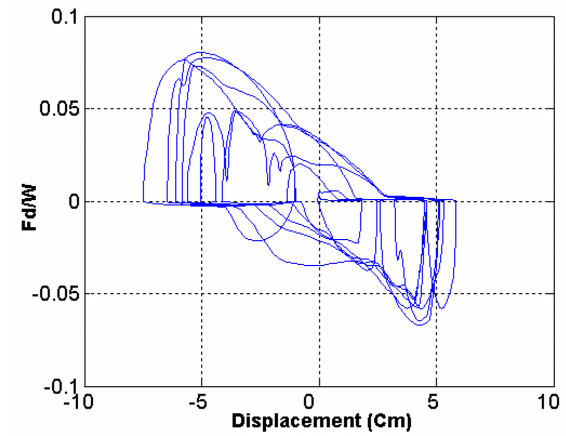

Figure 13) Artificial nonlinear damping force produced by PNS algorithm(El Centro 1940- 342 gal)

The maximum displacements of the base are 7.5, 9.0 and 7.5 centimeters in cases 1, 2 and 3, respectively. This result indicates that although PNS algorithm causes elongation of the natural period of the system (which can be suspected to large displacements), proper implementation of damping force results in both less accelerations and displacements. In other words, the variable artificial nonlinear damping force produced by the PNS algorithm causes larger hysteresis loop area in comparison with cases 1 and 2, more efficient energy dissipation.

Table 1) maximum base displacement U_{max} and base shear to weight ratio (El Centro 1940-342 gal & Kobe 1995-814 gal)

Ground motion	Case	U_{2max}(cm)	$F_{s\,max}/W$
El Centro 1940 342 gal	1	11	0.20
	2	15	0.14
	3	13	0.13
Kobe 1995 814 gal	1	0.13	0.18
	2	0.21	0.14
	3	0.13	0.13

As the second input ground motion, the Kobe 1995 record is applied. Figures 14 to 16 show the base shear- displacement loops of the structure in the three cases. Comparing three cases, It is shown that in case 1 the displacement has been controlled in the cost of increasing the load while in case 2, bilinear

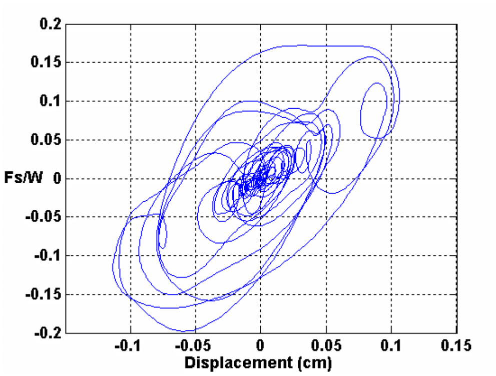

Figure 14) Hysteresis loop, Case 1
(Kobe 1995-814 gal)

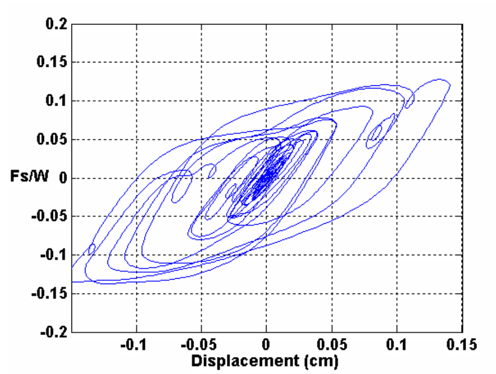

Figure 15) Hysteresis loop, Case 2
(Kobe 1995-814 gal)

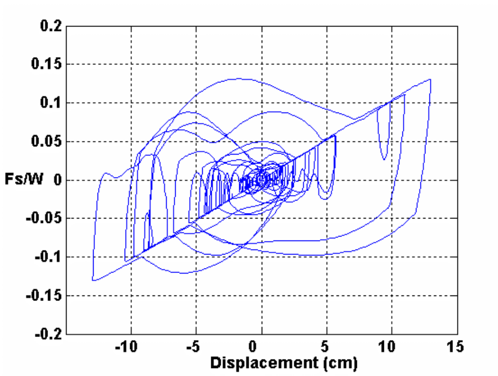

Figure 16) Hysteresis loop, Case 3
(Kobe 1995-814 gal)

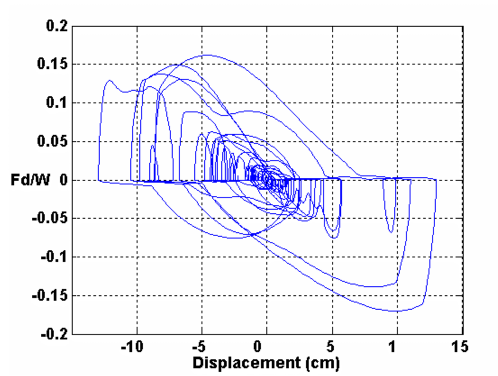

Figure 17) Artificial nonlinear damping force produced by PNS algorithm

Behavior of base isolation has controlled the force but increased the displacement. In case three, both displacement and force have been controlled in comparison with two other cases.
The results represented by the maximum displacement of the base U_{2max} and maximum ratio of base shear to weight $F_{s\,max}/W$ under El Centro 1940 and Kobe 1995 ground motions are summarized in Table 1.

COMPUTATION OF ENERGY COMPONENTS

In this section input energy and efficiency of energy dissipation in the three cases under El Centro ground motion are discussed.

Calculation of input energy and dissipated energy

The equation of motion for the system shown in Figure 2 can be written as:

$$M\ddot{U}(t) + C\dot{U}(t) + KU(t) = -M.A_g(t) + DF_d(t)$$

Where, M, C and K are mass, damping and stiffness matrices of the system. A_g is the ground acceleration vector. Here U denotes the displacement vector of the system such that: $U = \begin{Bmatrix} u_1 \\ u_2 \end{Bmatrix}$. The components of energy can be calculated by integrating this equation after multiplying by du [2]:

$$\int_0^u (M\ddot{U}(t))^T\, dU + \int_0^u (C\ddot{U}(t))^T\, dU + \int_0^u (K\ddot{U}(t))^T\, dU = \int_0^u (-M.A_g(t))^T\, dU + \int_0^u (DF_d)^T\, dU$$

The first three terms of the left side of this equation, represent kinetic energy (E_k), damping energy (E_d) and strain energy (E_s) respectively. Total cumulative input energy (E_i) is presented by the first component on the right side of this equation:

$$E_i = \int_0^u (-M.A_g(t))^{\mathrm{T}} \, dU$$

and, the second component on the right side represents the dissipated energy by variable damper (E_{var}):

$$E_{\mathrm{var}} = \int_0^u (DF_d)^T \, dU$$

Therefore the energy balance of the system takes place by the following relation:

$$E_i = E_k + (E_d + E_{\mathrm{var}}) + E_s$$

The impact of the sloshing liquid to the wall and roof of the tanks can cause problem in during earthquakes. In this study, to investigate the effect of each control system on the sloshing response, the vibration energy of convective mass of the liquid has been considered and compared.

To study the efficiency of energy dissipation in each case, a comparison between the input energy (Ei) and the dissipated energy (Ed) under the El Centro 1940 record NS component is performed, in particular the ratios of $\frac{E_d}{E_i}$ are investigated.

Figures 18, 19 and 20 show the accumulation of the input energy (E_i) and dissipated energy (E_d) in cases 1, 2 and 3, respectively. Based on the result of calculation, the ratios of $\frac{E_d}{E_i}$ are found to be 0.88, 0.93 and 0.96 in cases 1, 2 and 3, respectively. It follows that the case 3 achieves a good efficiency of energy dissipation comparing with two other cases.

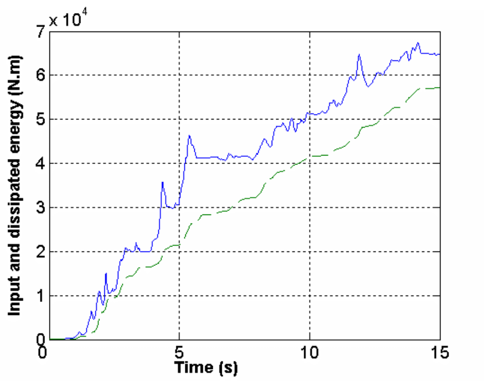

Figure 18) Input energy (E_i) and dissipated energy (E_d) in case 1

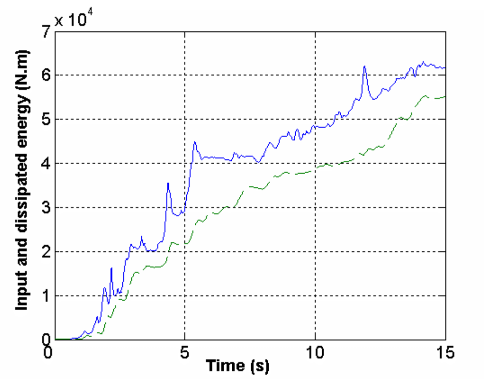

Figure 19) Input energy (E_i) and dissipated energy (E_d) in case 2

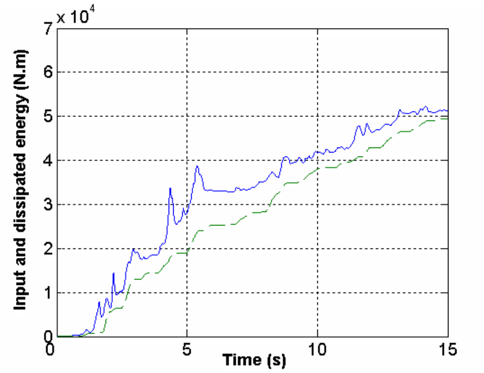

Figure 20) Input energy (E_i) and dissipated energy (E_d) in case 3

Calculation of Vibration Energy of Convective Mass

Figure 21 compares the vibration energy of convective mass of the liquid in the three cases under the El Centro excitation. The energy of the sloshing liquid during the earthquake causes direct and indirect damages to the tank structure and other facilities in industrial sites. The vibration energy of sloshing part which is the summation of kinetic and strain energy of convective of the convective mass, is compared as a measure of destruction potential of the sloshing part. The results are plotted in Figure 21. The peak value of the convective mass vibration energy is 2.05×10^4 and $1.60\ \times10^4$ and 1.39×10^4 in cases 1, 2 and 3, respectively. The successful energy dissipation of hybrid control system in case 3 provides transfer less energy to the superstructure which is expressed as the vibration energy.

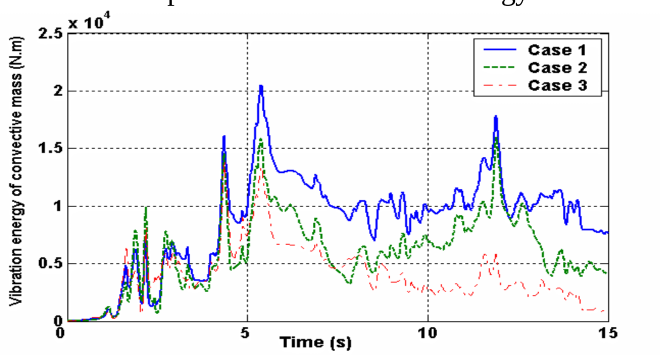

Figure 21) Vibration energy of convective mass (m_c) in three cases (El Centro 1940- 342 gal)

CONCLUSION

The behavior of cylindrical liquid storage tanks facilitated by different passive and hybrid passive and semi-active base isolation systems is studied. Reduction of base shear response with the application of isolation systems is confirmed. Application of PNS semi-active control algorithm to control the tank is found to be effective in the reduction of the base shear. Better performance of the PNS semi-active control in energy absorption is confirmed while comparing the ratio of dissipated energy to input energy in three cases. Vibration energy of the convective mass in the liquid part was compared as the measure to study the effect of response control systems in each case on the sloshing response of liquid. The results show that the PNS semi-active control case is the most effective system in reducing the vibration energy of the sloshing part in comparison with the other cases.

REFERENCES

1. A. S. Veletsos, P. Shivakumar, 1993, Sloshing response of layered liquids in rigid tanks, Earthquake engineering and structural dynamics 22, 801-821.
2. Akenori Shiwata, 1981, The latest seismic analysis; Mori kita publications (Japanese).
3. Haroun, M. A., 1983, Vibration studies and test of liquid storage tanks, Earthquake engineering and structural dynamics 11, 179-206.
4. Housner,G.W., 1963, Dynamic behavior of water tanks, Bulletin of seismological society of America 53, 381-387.
5. Iemura H., Igarashi A., and Nakata N., Full scale verification of tests of semi-active control of structures using variable joint damper system, Proceeding of the third world conference on structural control, Como, Italy, April 7~11 2002, pp 175~180.
6. Ko chi shin bun News paper, 18th Sep. 2003.
7. Kobori, T., Koshika, N., Yamada, K., and Ikeda, Y. 1991, Seismic response-controlled structure with active mass driver system, I: Design, Earthquake engineering and structural dynamics, 20(2), 133–149.
8. Pradono M. Harris, 2003, Seismic safety enhancement of cable-stayed bridges with pseudo negative stiffness dampers, Dissertation of Doctor course, Kyoto university.
9. Y. J. Park, Y. K. Wen and A. H-S. Ang, 1986, Random vibration of hysteretic systems under bi-directional ground motions, Earthquake engineering and structural dynamics 14, 543-557.
10. Yen Po Wang, Min-Cheng Teng and Kuo-whi Cheng, Seismic isolation of rigid cylindrical tanks using friction pendulum bearings, Earthquake engineering and structural dynamics, 30, 1083-1099.